Frame Time-Hopping Patterns in Multirate Optical CDMA Networks Using Conventional and Multicode Schemes

Amir R. Forouzan, *Student Member, IEEE*, Masoumeh Nasiri-Kenari, *Member, IEEE*, and Nasser Rezaee, *Member, IEEE*

***Abstract*—A class of generalized optical orthogonal codes (OOCs), namely, frame time-hopping (FTH) patterns with an extremely large cardinality, are studied for implementing multirate and multiservice (MR/MS) optical CDMA (OCDMA) networks. Conventional MR/MS methods, namely variable spreading rate and parallel mapping, are considered. Using FTH patterns, the problem of low OOC code cardinality in conventional MR/MS schemes is removed. Moreover, several new multicode methods, using subcode concatenation scheme, are proposed for MR/MS OCDMA. The proposed multicode schemes present flexibility for supporting MR/MS applications such as lower implementation complexity and cost, less need for service synchronization, and finally lower link power budget. Multiple-access performances of the systems are evaluated using saddle-point approximation methods considering photodetector shot-noise, dark current, and circuit thermal noise. The results show that the conventional parallel mapping outperforms the other schemes in high received powers, and the proposed multicode method, using Walsh subcode along with difference modulation, presents the best performance in low received powers for the cases considered.**

***Index Terms*—Frame time-hopping (FTH), multicode, multirate (MR), multiservice (MS), optical CDMA, optical orthogonal codes (OOCs), parallel mapping, subcode concatenation, variable spreading rate, Walsh code.**

I. INTRODUCTION

OPTICAL CDMA has attracted much interest for very fast fiber-optic (FO) and infrared wireless indoor multiple-access networks [1]–[4]. The desired features of optical CDMA in FO networks include simplicity in all optical implementation, minimum access delay, no need for scheduling protocols, higher security, and higher throughput [1]–[4]. A large and increasing amount of traffic over telecommunication networks is the bursty Internet traffic. Moreover, multimedia applications, which include different service types with time-variant data rates, have had a rapid growth in recent years. Therefore, multirate/multiservice (MR/MS) schemes for optical CDMA are of crucial importance for future all-optical networks.

Several authors have studied MR/MS schemes for optical CDMA based on optical orthogonal code (OOC) [5]–[10]. Two conventional MR/MS schemes are variable spreading rate and parallel mapping. In variable spreading rate or serial mapping [5]–[7], codes with variable-length codewords are employed. Codewords with smaller length are dedicated to services with higher bit rates, and codewords with larger length are dedicated to services with lower bit rates. Even though this scheme usually experiences a high bit error rate (BER) for high rate users, in [8], a multilength OOC code for multirate OCDMA is proposed which presents a lower BER for high rate users. In parallel mapping [9], more than one codeword is dedicated to users with high bit rate or more than one service. The number of codewords is proportional to user bit rate or number of its services. Previous studies have reported a poor performance for these two conventional schemes because they require large code cardinality, which is not feasible for OOC codes with good correlation properties. In order to obviate the problem of low code cardinality, in [10], a new MR/MS scheme is proposed, which is a combination of time-hopping CDMA and OOC codes. In this method, the transmission time is divided into slots and, as the data rate or number of active services of the user increases, more time slots are dedicated to the user to transmit its data using its allocated OOC codeword.

In [11], a class of generalized OOC is proposed which presents an extremely large cardinality and minimal degradation in performance compared to the optimal OOC codes, *i.e.*, OOC with correlation functions bounded by one (OOC ($\lambda = 1$)). This scheme is also a type of time-hopping CDMA and the proposed codes are called frame time-hopping (FTH) patterns. In this paper, we consider variable spreading rate and parallel mapping schemes for MR/MS optical CDMA networks using FTH patterns as user signature sequences. We also consider multicode schemes using subcode concatenation method for both binary pseudonoise (PN) and orthogonal Walsh sequences. Subcode concatenation method was first proposed for radio DS-CDMA [12]. Furthermore, we modify the multicode scheme for performance enhancement. The multicode scheme presents high flexibility for supporting MR/MS applications such as simpler coordination protocols, simpler service synchronization, lower implementation complexity and cost, and finally lower link budget. We evaluate the performance of the

Paper approved by W. C. Kwong, the Editor for Optical Communications of the IEEE Communications Society. Manuscript received July 9, 2004; revised November 7, 2004.

A. R. Forouzan was with the Electrical and Computer Engineering Department, University of Tehran, Tehran, Iran. He is now with the Department of Electrical and Computer Engineering, University of Canterbury, Christchurch 8005, New Zealand (e-mail: a.forouzan@elec.canterbury.ac.nz).

M. Nasiri-Kenari is with the Department of Electrical Engineering, Sharif University of Technology, Tehran 11365-9363, Iran (e-mail: mnasiri@sharif.ac.ir).

N. Rezaee is with the Electrical and Computer Engineering Department, University of Tehran, Tehran 14399, Iran.

Digital Object Identifier 10.1109/TCOMM.2005.847130

proposed schemes considering the main sources of noise in FO networks. Numerical results show that the conventional parallel mapping scheme achieves a considerable performance using frame time-hopping generalized OOCs, which is in contrast with the results previously reported using OOC ($\lambda = 1$). The results also show that the newly proposed multicode scheme with Walsh subcode and difference modulation is the superior method when the received power is low.

This paper is organized as follows. In Section II, we describe the considered MR/MS schemes including the transmitting waveform and receiver structure. In Section III, we evaluate the performance of the schemes. In Section IV, we present some numerical results, and we conclude this paper in Section V.

II. System Description

A. Serial Mapping Using Variable Spreading Rate

The simplest solution for simultaneously transmitting several service data streams, from a physical layer point of view, is combining data streams of all the services of the user in higher network layers to obtain a single data stream, namely, accumulated data stream of the user and then transmitting this data stream employing a single service scheme. The rate of accumulated data stream is at least the sum of data rates of the active services of the user.[1] Based on frame time-hopping (FTH) patterns and binary pulse position modulation (BPPM), the transmitted signal power of user k ($1 \leq k \leq M$) is written as [11]

$$p_{tr}^{(k)}(t) = \sum_{j=-\infty}^{+\infty} p_{T_w}\left(t - jT_f - c_j^{(k)}T_c - \frac{d_j^{(k)}T_c}{2}\right) \quad (1)$$

where j is the frame or pulse index number, T_c and T_f are the chip and frame time durations, respectively, and $p_{T_w}(\cdot)$ is the transmitting pulse with duration $T_w \leq T_c/2$. $\left\{c_j^{(k)}\right\}$ is the time-hopping pseudorandom (TH-PN) sequence of user k, which uniformly take on an integer value in the interval $[0, N_h)$, where $N_h = \lfloor T_f/T_c \rfloor$ is the number of hop positions in a frame time. More precisely, $c_j^{(k)}$ determines the marked chip in frame j where the pulse is transmitted in by user k. $\left\{d_j^{(k)}\right\}$ is the binary sequence of the transmitted symbols of user k. Consider $\left\{D_i^{(k)}\right\}$, ($D_i^{(k)} \in \{0,1\}$), as the accumulated data stream of user k. Then, $\left\{d_j^{(k)}\right\}$ is w repetitions of $\left\{D_i^{(k)}\right\}$, i.e., $d_j^{(k)} = D_i^{(k)}$ for $iw \leq j < (i+1)w$. For BPPM modulation considered, each chip interval is divided into two time slots. When $d_j^{(k)}$ is "zero," the pulse is transmitted in the first slot of the marked chip in frame j, and when it is "one" the pulse is transmitted in the second slot of the marked chip. The accumulate data rate of user k is computed by $R_s = 1/(wT_f)$. Therefore, in an MR/MS network, in which R_s is not a fixed number, w must vary adaptively to meet the required instant data rate, which demands a variable spreading rate. We assume that this process is achieved by the means of protocols in higher layers of the network. In single-service FTH networks, $\left\{c_j^{(k)}\right\}$ is periodic with period w [11]. However, for MR/MS applications, for the simplicity of user-receiver synchronization and higher code cardinality, we assume that $\left\{c_j^{(k)}\right\}$ is periodic with a fixed period N_p independent of w, i.e., $c_j^{(k)} = c_{j+N_p}^{(k)}$. In this case, users can change their data rate without losing synchronization, as the TH-PN sequence remains unchanged. Moreover, code cardinality will be about $(N_h)^{N_p-1}/N_p$, which is extremely large for moderate values of N_p and N_h. As a result, FTH patterns easily lend themselves for the variable spreading rate scheme, while a specific code design is required in general for OOC patterns [8].

[1]In order to separate the services at the receiver side, some differentiating bits must be added to the accumulated data stream, which we neglect in this paper.

Assuming perfect power control, the received signal at the output of photodetector of user 1 (desired user) can be written as

$$r(t) = A\sum_{k=1}^{M} p_{tr}^{(k)}(t - \tau_k) + n(t) \quad (2)$$

where A is the attenuation factor due to fiber and the optical star-coupler loss, M is the number of active users, τ_k is the delay of user k, and $n(t)$ is the received noise, including circuit thermal noise and photodetector dark current.

In this study, we consider the well-known correlator receiver [11, (9)]. The decision rule for detecting ith bit of user $1 (D_i^{(1)})$ is

$$u = \sum_{j=iw}^{(i+1)w-1} \alpha_j \underset{D_i^{(1)}=1}{\overset{D_i^{(1)}=0}{\gtrless}} 0 \quad (3)$$

where u is the correlator output or decision variable and

$$\alpha_j = \int_{\tau_1+jT_f}^{\tau_1+(j+1)T_f} r(t)v(t - \tau_1 - jT_f - c_j^{(1)}T_c)dt \quad (4)$$

is the j^{th} pulse correlator output and $v(t) \triangleq p_{T_w}(t) - p_{T_w}(t - T_c/2)$ is called the receiver's template signal.

B. Parallel Mapping

Another popular method to implement MR/MS O-CDMA is parallel mapping. In this method, each service is treated as a distinct user. Therefore, an OOC code with cardinality as large as the maximum number of services of the network is required. Previous studies on parallel mapping has considered OOC codes with autocorrelation and cross-correlation values bounded by one, i.e., OOC ($\lambda = 1$), which have a low cardinality. As a result, the authors have reported that parallel mapping is not suitable for MR/MS O-CDMA. In this study, however, we consider FTH generalized OOC codes with extremely large cardinality [11].

The signal waveform and receiver structure are as in single-rate/single-service FTH-OCDMA networks [11]. The transmitted signal due to service q of user k can be written as

$$p_{tr}^{(k,q)}(t) = \sum_{j=-\infty}^{+\infty} p_{T_w}\left(t - jT_f - c_j^{(k,q)}T_c - \frac{d_j^{(k,q)}T_c}{2}\right) \quad (5)$$

where $\left\{d_j^{(k,q)}\right\}$ and $\left\{c_j^{(k,q)}\right\}$ are the sequence of transmitting symbols and the dedicated TH-PN sequence of service q of user k, respectively. As before, $\left\{d_j^{(k,q)}\right\}$ is w repetitions of the binary data sequence of the service, that is, $d_j^{(k,q)} = D_i^{(k,q)}$ for $iw \leq j < (i+1)w$. Here, we assume that w is a fixed number and service with higher rates is supported by assigning more than one TH-PN code to the service.

The structure of correlation receiver for detecting the desired service, which we consider to be the first service of user 1 ($D_i^{(1,1)}$), is the same as (3), and is obtained by substituting $\left\{c_j^{(1)}\right\}$ by $\left\{c_j^{(1,1)}\right\}$ in (4).

C. Multicode Using PN Subcode Concatenation Scheme

In this novel method, a single FTH codeword (TH-PN sequence) is assigned to each user such that all the services of the user utilize the same marked chips for sending their pulses. To separate different services of the user, a second binary PN code (called subcode) with length w is dedicated to each service. Suppose $\left\{C_j^{(k,q)}\right\}$ is the binary PN sequence of the q^{th} service of user k and $\left\{d_j^{(k,q)}\right\}$ is the sequence of transmitting symbols of this service. As before, $\left\{d_j^{(k,q)}\right\}$ is w repetitions of binary data bits of this service ($\left\{D_i^{(k,q)}\right\}$). On the other hand $\left\{C_j^{(k,q)}\right\}$ is a periodic sequence with period w, i.e., $C_j^{(k,q)} = C_{j+nw}^{(k,q)}$ for any integer n. The subcode determines the location for sending the symbols "zero" and "one" in the first and second slots of each of w marked chips of the service in the following way: When $C_j^{(k,q)}$ is "zero" the first slot of the marked chip j is used to transmit bit "zero" and the second slot is used for bit "one." When $C_j^{(k,q)}$ is "one," however, the first slot of the marked chip is used to transmit bit "one" and the second slot for bit "zero." Therefore, using the binary operator XOR ($\oplus$), the transmitted signal of the qth service of user k can be written as

$$p_{tr}^{(k,q)}(t)=\sum_{j=-\infty}^{\infty} p_{T_w}\left(t-jT_f-c_j^{(k)}T_c-\frac{\left(C_j^{(k,q)}\oplus d_j^{(k,q)}\right)T_c}{2}\right). \tag{6}$$

Since all of the services of user k use the same FTH pseudorandom sequence ($\left\{c_j^{(k)}\right\}$), the total signal transmitted by user k can be easily written as (7), shown at the bottom of the page, where $m_j^{(k)} = \sum_{q=1}^{N^{(k)}}\left(1 - C_j^{(k,q)}\oplus d_j^{(k,q)}\right)$ and $n_j^{(k)} = \sum_{q=1}^{N^{(k)}} C_j^{(k,q)} \oplus d_j^{(k,q)} = N^{(k)} - m_j^{(k)}$ are the total power transmitted by all the services of user k in the first and second slots of the jth marked chip, respectively, and $N^{(k)}$ is the number of active services of the user.

Conditioned on the transmitted data bit of the desired service (service 1 of user 1), i.e., $D_i^{(1,1)}$, being "zero" and "one," the transmitted signal waveform is $\sum_{j=iw}^{(i+1)w-1} p_{T_w}\left(t - jT_f - c_j^{(1)}T_c - C_j^{(1,1)}T_c/2\right)$ and $\sum_{j=iw}^{(i+1)w-1} p_{T_w}\left(t - jT_f - c_j^{(1)}T_c - \overline{C_j^{(1,1)}}T_c/2\right)$, respectively, where $\overline{C_j^{(1,1)}} = C_j^{(1,1)} \oplus 1$. Therefore, the decision rule for the correlation receiver for detecting $D_i^{(1,1)}$ is (8), shown at the bottom of the page. After some algebraic simplification, the above equation can be written as

$$u = \sum_{j=iw}^{(i+1)w-1} (-1)^{C_j^{(1,1)}} \alpha_j \underset{D_i^{(1,1)}=1}{\overset{D_i^{(1,1)}=0}{\gtrless}} 0 \tag{9}$$

where u is the correlator output or decision variable and α_j is as defined in (4). As α_j's are obtained once [from (4)] for detecting the bits of all services of the user based on (9), the receiver complexity for this scheme will be the same as that of the conventional variable spreading rate scheme and much lower than that of the parallel mapping method described in Section II-B, in which α_j's, the pulse correlator outputs, must be obtained for each service separately.

The multicode scheme is superior to the variable spreading rate scheme in the sense that the services of any user are sent independently and there is minimum need for coordination protocols when the service turns on or off. Compared to parallel mapping scheme, described in Section II-B, this scheme can be implemented using much fewer laser sources and requires only one pulse correlator to detect all services of the user. Furthermore, in the parallel mapping scheme, synchronization is required each time a service turns on, while in the multicode scheme at the time a service turns on, the synchronization is needed only when all the services of the user are inactive.

$$p_{tr}^{(k)}(t) = \sum_{j=-\infty}^{\infty} m_j^{(k)} p_{T_w}\left(t - jT_f - c_j^{(k)}T_c\right) + n_j^{(k)} p_{T_w}\left(t - jT_f - c_j^{(k)}T_c - \frac{T_c}{2}\right) \tag{7}$$

$$\int_{t=\tau_1+iwT_f}^{\tau_1+(i+1)wT_f} r(t) \sum_{j=iw}^{(i+1)w-1} p_{T_w}\left(t - jT_f - c_j^{(1)}T_c - \frac{C_j^{(1,1)}T_c}{2}\right)\mathrm{d}t \underset{1}{\overset{0}{\gtrless}} \int_{t=\tau_1+iwT_f}^{\tau_1+(i+1)wT_f} r(t) \sum_{j=iw}^{(i+1)w-1} p_{T_w}\left(t - jT_f - c_j^{(1)}T_c - \frac{\overline{C_j^{(1,1)}}T_c}{2}\right)\mathrm{d}t \tag{8}$$

D. Multicode Using Walsh Subcode Concatenation Scheme

As we demonstrate later in numerical results section, the method of Section II-C, despite all of its advantages, shows a poor multiservice performance due to high mutual interference between services of a user. To reduce the mutual interference between services, we suggest employing orthogonal Walsh code instead of binary PN subcode. Consider $\vec{v} = (v_1, v_2, \ldots, v_n)$ and $\vec{u} = (u_1, u_2, \ldots, u_n)$ $(u_j, v_j \in \{0, 1\})$ as two codewords of a Walsh code with length n. The orthogonality property of Walsh code states that

$$\langle \vec{v}, \vec{u} \rangle \triangleq \sum_{j=1}^{n} (-1)^{v_j} (-1)^{u_j} = \begin{cases} n, & \vec{v} = \vec{u} \\ 0, & \text{otherwise.} \end{cases} \quad (10)$$

Walsh code exists only in lengths that are power of 2. The cardinality of a Walsh code with length w is w. Therefore, when a FTH pattern with weight w is used, the number of services of each user is at most w. Suppose $\left\{W_j^{(k,q)}\right\}$ is the binary Walsh sequence dedicated to service q of user k. The transmitted signal of this service can be written as

$$p_{tr}^{(k,q)}(t) = \sum_{j=-\infty}^{\infty} p_{T_w}\left(t - jT_f - c_j^{(k)} T_c - \frac{\left(W_j^{(k,q)} \oplus d_j^{(k,q)}\right) T_c}{2}\right). \quad (11)$$

Similarly, the total transmitted signal of user k can be written in the form of (7), in which $m_j^{(k)}$ and $n_j^{(k)}$ are given by $m_j^{(k)} = \sum_{q=1}^{N^{(k)}} \left(1 - W_j^{(k,q)} \oplus d_j^{(k,q)}\right)$ and $n_j^{(k)} = \sum_{q=1}^{N^{(k)}} W_j^{(k,q)} \oplus d_j^{(k,q)}$. The decision rule of the correlation receiver is written as

$$u = \sum_{j=iw}^{(i+1)w-1} (-1)^{W_j^{(1,1)}} \alpha_j \underset{D_i^{(1,1)}=1}{\overset{D_i^{(1,1)}=0}{\gtrless}} 0 \quad (12)$$

where α_j is the jth pulse correlator output defined in (4).

E. Multicode Using Walsh Subcode and Difference Modulation

As can be seen from (4) and (12), the receiver subtracts the signal received in the second slot of each marked chip from the signal received in the first slot of the marked chip and then employs these w values to detect the transmitted bit. That is the absolute value of the signal transmitted in the first and second slots of the marked chips (i.e., $m_j^{(k)}$ and $n_j^{(k)}$) are not directly employed in decision process. In fact, their difference values are used in decision variable. Therefore, instead of transmitting the absolute value of signal in the first and second slots of the marked chips as in (7), we suggest transmitting their difference as follows:

$$p_{tr}^{(k)}(t) = \sum_{j=-\infty}^{+\infty} \text{abs}(\delta_j^{(k)}) p_{T_w}\left(t - jT_f - c_j^{(k)} T_c - \frac{\text{sgn}(\delta_j^{(k)}) T_c}{2}\right) \quad (13)$$

where

$$\delta_j^{(k)} = n_j^{(k)} - m_j^{(k)} \quad (14)$$

and the sign function, $\text{sgn}(x)$, is defined as

$$\text{sgn}(x) \triangleq \begin{cases} 1, & x > 0 \\ 0, & \text{otherwise.} \end{cases} \quad (15)$$

As it can be realized, when $m_j^{(k)}$ is greater than $n_j^{(k)}$, $\delta_j^{(k)}$ is negative and $\text{sgn}\left(\delta_j^{(k)}\right)$ is zero. Therefore, a pulse with power $m_j^{(k)} - n_j^{(k)}$ is transmitted in the first slot of the marked chip and nothing is sent in the second slot. As a result, the difference of the transmitted signal in the first and second slots of the marked chip remains unchanged. Similarly, for $m_j^{(k)}$ less than $n_j^{(k)}$, a pulse with power $n_j^{(k)} - m_j^{(k)}$ is transmitted in the second slot. Finally, for $\delta_j^{(k)}$ equal to zero, no pulse is transmitted in either slot. This method has a few advantages over the previous method. The most obvious advantage is the less link power budget. There is also less multiple-access interference in the network. Moreover, while the desired signal remains unchanged, there is less shot-noise in receiver, as the shot-noise is proportional to the received power. The structure of the correlation receiver is the same as the previous method, which is formulated in (12) and (4).

Fig. 1 illustrates a possible transmitter structure for each MR/MS signaling method described earlier. An example of the transmitted signal for each scheme is presented in Fig. 2.

III. Performance Analysis

In this section, we provide the performance analysis of the above described MR/MS schemes in ideal and general cases. In the ideal case, the photodetector shot-noise and dark current and the circuit thermal noise are not taken into account, while in the general case we consider their effects. We assume a chip-synchronous system [2]. To evaluate the system performance, we employ saddle-point approximation techniques [13]. Using saddle-point approximation techniques, only computation of the probability characteristic function (CF) of the correlator output (decision variable) is required, which is usually much simpler than computing the probability cumulative density function at a threshold value.

We consider that there are M active users in the network each with $N^{(k)}$ ($k = 1$ to M) similar services, where k indicates the user index number. We consider a perfect power control among services in the network, i.e., the energy received per bit from each *service* is the same for all of the active services in the network. To obtain the CF of the output of the correlator matched to the desired service (service 1 of user 1), from (3) we note that the correlator output (u) is the sum of a few independent components, namely, desired user signal, multiple-access interference, photodetector dark current, and circuit thermal noise, and as a result its CF, i.e., $\Phi(s)$, is the product of CFs of these components

$$\Phi(s) = \Phi^{(1)}(s) \, \Phi_{MA}(s) \, \Phi_d(s) \, \Phi_n(s) \quad (16)$$

where $\Phi^{(1)}(s)$, $\Phi_{MA}(s)$, $\Phi_d(s)$, and $\Phi_n(s)$ are the CFs of the desired user signal, multiple-access interference, photodetector

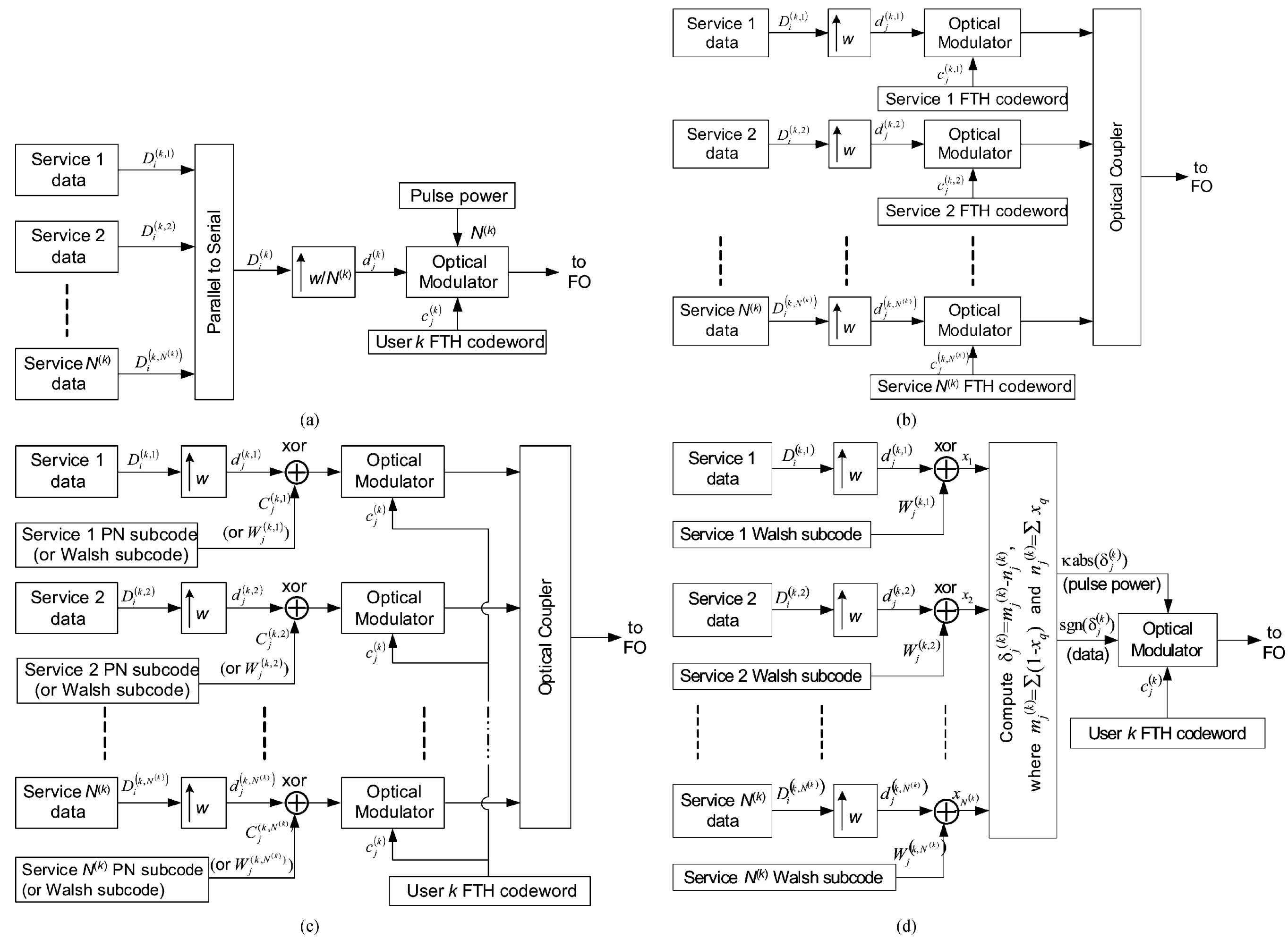

Fig. 1. Transmitter structure for the proposed schemes. (a) Serial mapping. (b) Parallel mapping. (c) Multicode using PN subcode (or Walsh subcode). (d) Multicode using Walsh subcode and difference modulation.

dark current, and circuit thermal noise, respectively. Since the signals from interfering users are independent, we have

$$\Phi_{MA}(s) = \prod_{k=2}^{M} \Phi^{(k)}(s) \tag{17}$$

where $\Phi^{(k)}(s)$ is the CF of the interference component due to user k. We need to evaluate the terms $\Phi^{(1)}(s)$, $\Phi^{(k)}(s)$, $\Phi_d(s)$, and $\Phi_n(s)$ to obtain $\Phi(s)$. In the following, we evaluate these terms for each MR/MS schemes in both ideal and general cases. Note that, in the ideal case, the dark current and circuit thermal noise terms ($\Phi_d(s)$ and $\Phi_n(s)$) are neglected.

With BPPM modulation, the probability of error is equal to probability of error conditioned on the desired service bit, i.e., $D_i^{(1,1)}$. Therefore, in the following, without loss of generality, we assume $D_i^{(1,1)} = 0$. In this case, error occurs when the correlator output is less than "0" [see (3), (9), and (12)]. Then, the bit error rate (BER) can be evaluated almost precisely from the CF of the decision variable using the saddle-point approximation technique as follows [13]:

$$\Pr\left\{u < 0 \mid D_0^{(1,1)} = 0\right\} \approx \frac{\Phi(s_0)}{\left(|s_0|\sqrt{2\pi\Psi''(s_0)}\right)} \tag{18}$$

where $\Phi(s)$ is the CF of the decision variable u conditioned on the transmitted data bit of the desired service being "zero," $\Psi(s) \triangleq \ln(\Phi(s)/|s|)$, $\Psi''(s) \triangleq \partial^2\Psi(s)/\partial s^2$, and s_0 is the negative root of equation $\Psi'(s) \triangleq \partial\Psi(s)/\partial s = 0$.

In general case, we suppose that the mean received photoelectron count per service bit is m_b, the mean dark-current photoelectron count per pulse is m_d, and the normalized standard division of thermal noise component at the pulse correlator output is σ_n. The mean received photoelectron count per pulse with amplitude "one" for the first four methods is simply evaluated as $m_r = m_b/w$. For the Walsh and subtract methods, however, the mean received photoelectron count per pulse is a nontrivial function of the number of active services of the user, which will be evaluated later in the numerical results section.

A. Serial Mapping

In this case, for each user k with $N^{(k)}$ active services, the effective FTH code weight (or the number of pulses per bit for each service of this user) is $w/N^{(k)}$. On the other hand, the pulse energies are multiplied by $N^{(k)}$ because of the perfect power control assumption. Therefore, the CFs can be simply evaluated using the results obtained in [11] for single-rate/single-service FTH-FO-CDMA networks as follows.

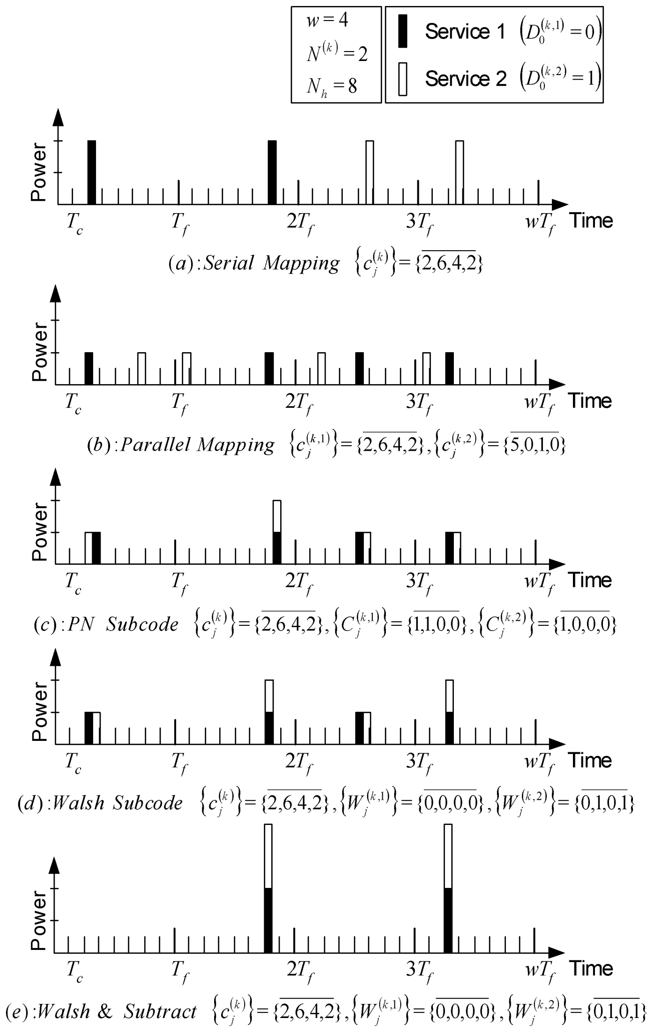

Fig. 2. Transmitted signal in a bit duration in the proposed schemes and corresponding parameters assuming an energy per service-bit of four.

Ideal Case:

$$\Phi^{(1)}(s) = \exp(ws) \text{ and} \tag{19}$$

$$\Phi^{(k)}(s) = \left(\alpha + \frac{1}{2}\beta\left[\exp\left(N^{(k)}s\right) + \exp\left(-N^{(k)}s\right)\right]\right)^{w/N^{(1)}} \tag{20}$$

where $\alpha = 1 - T_c/T_f$, and $\beta = T_c/T_f$.

General Case:

$$\Phi^{(1)}(s) = \exp\left(wm_r\left(e^s - 1\right)\right) \tag{21}$$

$$\Phi^{(k)}(s) = \left(\alpha + \frac{1}{2}\beta\left[\exp\left(N^{(k)}m_r(e^s - 1)\right) + \exp\left(N^{(k)}m_r(e^{-s} - 1)\right)\right]\right)^{w/N^{(1)}} \tag{22}$$

$$\Phi_d(s) = \exp\left(\frac{wm_d}{N^{(1)}}\left(e^s + e^{-s} - 2\right)\right) \tag{23}$$

and

$$\Phi_n(s) = \exp\left(-\frac{N^{(1)}s^2}{4w\sigma_n^2}\right). \tag{24}$$

B. Parallel Mapping

The results in [11] are applicable in this case as well. Note that the interference components due to undesired services of user one and the services of all interfering user k can be well considered *i.i.d* variables. Then, from [11], the CF's are given as:

Ideal Case:

$$\begin{aligned}\Phi^{(1)}(s) &= \Phi^{(1,1)}(s)\prod_{q=2}^{N^{(1)}}\Phi^{(1,q)}(s)\\ &= \exp(ws)\left(\alpha + \frac{1}{2}\beta(\exp(s) + \exp(-s))\right)^{w\left(N^{(1)}-1\right)}\end{aligned} \tag{25}$$

where $\Phi^{(1,1)}(s)$ is the CF of the desired service component, and $\Phi^{(1,q)}(s)$ is the CF of service q of user one component at the output of correlator. Also, we have

$$\begin{aligned}\Phi^{(k)}(s) &= \prod_{q=1}^{N^{(k)}}\Phi^{(k,q)}(s)\\ &= \left(\alpha + \frac{1}{2}\beta\left(\exp(s) + \exp(-s)\right)\right)^{wN^{(k)}}\end{aligned} \tag{26}$$

where $\Phi^{(k,q)}(s)$ is the CF of service q of user k term at the correlator output.

General Case:

$$\Phi^{(1)}(s) = \exp\left(wm_r\left(e^s - 1\right)\right)\left(\alpha + \frac{1}{2}\beta(\exp(m_r(e^s - 1)) + \exp(m_r(e^{-s} - 1)))\right)^{w\left(N^{(1)}-1\right)} \tag{27}$$

$$\Phi^{(k)}(s) = \left(\alpha + \frac{1}{2}\beta\left(\exp\left(m_r\left(e^s - 1\right)\right) + \exp\left(m_r\left(e^{-s} - 1\right)\right)\right)\right)^{wN^{(k)}} \tag{28}$$

$$\Phi_d(s) = \exp\left(wm_d\left(e^s + e^{-s} - 2\right)\right) \tag{29}$$

and

$$\Phi_n(s) = \exp\left(-\frac{s^2}{4w\sigma_n^2}\right). \tag{30}$$

C. Multicode Using PN Subcode Concatenation Scheme

Ideal Case: Without loss of generality, we assume that $\tau_1 = 0$, $c_j^{(1)} = 0$ [14], and $C_j^{(1,1)} = 0$, and as before we consider detection of bit "zero" (i.e., $i = 0$). In this case (9) reduces to

$$u = \int_{t=0}^{wT_f} r(t)\sum_{j=0}^{w-1}p_{T_w}(t - jT_f)\,\mathrm{d}t - \int_{t=0}^{wT_f} r(t)\sum_{j=0}^{w-1}p_{T_w}\left(t - jT_f - \frac{T_c}{2}\right)\mathrm{d}t \underset{1}{\overset{0}{\gtrless}} 0 \tag{31}$$

and the desired signal in the interval of interest is $A\sum_{j=0}^{w-1} p_{T_w}(t-jT_f)$. Therefore, the desired signal component at the output of correlator is w, with CF equal to $\Phi^{(1,1)}(s) = \exp(ws)$. Each pulse of an undesired service q $(2 \leq q \leq N^{(1)})$ of user one (e.g., $p_{T_w}\left(t-jT_f-\left(d_j^{(1,q)}\oplus C_j^{(1,q)}\right)T_c/2\right)$), which uses the same marked chip as the desired service in the same frame, has the effect of "1" or "−1" at the output of correlator, conditioned on the value $C_j^{(1,q)}\oplus d_j^{(1,q)}$ being "zero" or "one," respectively. As $C_j^{(1,q)}$ selects "zero" and "one" randomly and with equal probability 1/2, and $d_j^{(1,q)}$ is constant during w frames of a bit, each undesired service of user one, has a binomial distribution at correlator output with CF equal to

$$\Phi^{(1,q)}(s) = \left(\frac{\exp(s)}{2}+\frac{\exp(-s)}{2}\right)^w. \tag{32}$$

Therefore, we have

$$\Phi^{(1)}(s) = \exp(ws)\left(\frac{\exp(s)}{2}+\frac{\exp(-s)}{2}\right)^{w\left(N^{(1)}-1\right)}. \tag{33}$$

Now we compute $\Phi^{(k)}(s)$ $(k>1)$. We denote the CF of the interference term due to user k in frame j by $\Phi_j^{(k)}(s)$. By calling the event that the marked chip of user k in frame j coincides with that of user 1 as a "hit," the probability of a hit is equal to $\beta = 1/N_h = T_c/T_f$, and the probability of "no hit" is $\alpha = 1-\beta$ [11]. Therefore

$$\Phi_j^{(k)}(s) = \alpha\Phi_{j|\text{no hit}}^{(k)}(s) + \beta\Phi_{j|\text{hit}}^{(k)}(s). \tag{34}$$

It can be simply shown that $\Phi_{j|\text{no hit}}^{(k)}(s) = 1$ and $\Phi_{j|\text{hit}}^{(k)}(s) = (\exp(s)/2+\exp(-s)/2)^{N^{(k)}}$. Finally, noting that the interference components due to each user k in w frames corresponding to each bit are i.i.d variables, we obtain

$$\Phi^{(k)}(s) = \left(\alpha+\beta\left(\frac{e^s}{2}+\frac{e^{-s}}{2}\right)^{N^{(k)}}\right)^w. \tag{35}$$

General Case: To evaluate $\Phi^{(1)}(s)$ and $\Phi^{(k)}(s)$ when considering the photodetector shot-noise, we need simply substitute $\exp(s)$ with $\exp(m_r(e^s-1))$ and $\exp(-s)$ with $\exp(m_r(e^{-s}-1))$ in the results obtained in the Ideal Case. Thus

$$\Phi^{(1)}(s) = \exp(wm_r(e^s-1))\left(\frac{1}{2}\exp(m_r(e^s-1)) + \frac{1}{2}\exp\left(m_r\left(e^{-s}-1\right)\right)\right)^{w\left(N^{(1)}-1\right)} \tag{36}$$

$$\Phi^{(k)}(s) = \left(\alpha+\beta\left(\frac{1}{2}\exp(m_r(e^s-1)) + \frac{1}{2}\exp\left(m_r\left(e^{-s}-1\right)\right)\right)^{N^{(k)}}\right)^w. \tag{37}$$

The CF of dark-current and thermal noise components are the same as those derived for parallel mapping scheme [(29) and (30)].

D. Multicode Using Walsh Subcode Concatenation Scheme

Ideal Case: Similar to the previous scheme, the CF of the desired service is computed as $\Phi^{(1,1)}(s) = \exp(ws)$. To compute the CF of undesired services of user 1, we consider service q $(q\neq 1)$ of user 1. For any arbitrary frame j, when $W_j^{(1,1)}$ and $W_j^{(1,q)}$ are equal, a "1" is added to the correlator output, and when they are unequal a "−1" is added to the correlator output. Therefore, in either case, the product $(-1)^{W_j^{(1,1)}}(-1)^{W_j^{(1,q)}}$ is added to the correlator output. Therefore, the total effect of an arbitrary service q of user one in a correlator output is

$$\sum_{j=0}^{w-1}(-1)^{W_j^{(1,1)}}(-1)^{W_j^{(1,q)}} = 0 \tag{38}$$

where the last equality is obtained from (10). Consequently,

$$\Phi^{(1)}(s) = \exp(ws). \tag{39}$$

$\Phi^{(k)}(s)$ is calculated to be the same as $\Phi^{(k)}(s)$ for the previous scheme, obtained in (35). However, for this scheme, we can relax the previous assumption of chip-synchronous networks to half-chip synchronous networks in which we have

$$\tau_k - \tau_1 = \frac{nT_c}{2} \tag{40}$$

where n is an integer. Using this assumption, we simply obtain

$$\Phi^{(k)}(s) = \left(\alpha+\frac{1}{2}\beta\left(\left(\frac{1}{2}+\frac{\exp(s)}{2}\right)^{N^{(k)}} + \left(\frac{\exp(s)}{2}+\frac{\exp(-s)}{2}\right)^{N^{(k)}} + \left(\frac{1}{2}+\frac{\exp(-s)}{2}\right)^{N^{(k)}} - 1\right)\right)^w. \tag{41}$$

General Case: In contrast to the Ideal Case, when photodetector shot-noise is taken into account, the effect of undesired services of user one does not cancel out. To evaluate the CF of service q of user one, we note that, conditioned on the product $(-1)^{W_j^{(1,1)}}(-1)^{W_j^{(1,q)}}$ being "1" or "−1," the pulse of service q in frame j causes a Poisson photon count with mean m_r or a negative of a Poisson photon count with mean $-m_r$ at the pulse correlator output, respectively. Since the product $(-1)^{W_j^{(1,1)}}(-1)^{W_j^{(1,q)}}$ has the value either "1" or "−1", from (38) we conclude that the number of occurrence of "1" and "−1" is equal to $w/2$. Therefore,

$$\begin{aligned}\Phi^{(1,q)}(s) &= [\exp(m_r(e^s-1))]^{w/2}\left[\exp\left(m_r\left(e^{-s}-1\right)\right)\right]^{w/2} \\ &= \exp\left(wm_r\left(\frac{e^s+e^{-s}}{2}-1\right)\right).\end{aligned} \tag{42}$$

Since the CF of the term due to the desired service is $\Phi^{(1,1)}(s) = \exp(wm_r(e^s-1))$, considering $N^{(1)}-1$ undesired active services for user 1, we have

$$\Phi^{(1)}(s) = \exp(wm_r(e^s-1))\exp\left(wm_r\left(\frac{e^s+e^{-s}}{2}-1\right)\right). \tag{43}$$

Again, the CFs of the terms due to dark current and thermal noise are the same as those of parallel mapping scheme [(29) and (30)]. Also, for $\Phi^{(k)}(s)$, we simply need to substitute $\exp(s)$ by $\exp(m_r(e^s-1))$ and $\exp(-s)$ by $\exp(m_r(e^{-s}-1))$ in the results obtained in Ideal Case, i.e., (35) and (41) for synchronous and half-chip synchronous networks, respectively.

E. Multicode Using Walsh Subcode and Difference Modulation

Ideal Case: Without loss of generality, again we consider detection of bit "zero," i.e., $i=0$, and $\tau_1=0$. In the Ideal Case, the effect of the desired user's signal at the output of correlator is given in the equation shown at the bottom of the page. Considering the pulse, chip, and frame durations, we simply obtain (44), shown at the bottom of the page. The term I in (44) can be rewritten as

$$\begin{aligned} I &= A\,\mathrm{abs}\left(\delta_j^{(1)}\right) \times\int_{t=0}^{T_c} p_{T_w}\left(t-\frac{\mathrm{sgn}\left(\delta_j^{(1)}\right)T_c}{2}\right)\left(p_{T_w}(t)-p_{T_w}\left(t-\frac{T_c}{2}\right)\right)dt \\ &= A\,\mathrm{abs}\left(\delta_j^{(1)}\right) \times\int_{t=0}^{T_c} p_{T_w}\left(t-\frac{\mathrm{sgn}\left(\delta_j^{(1)}\right)T_c}{2}\right)p_{T_w}(t)\,dt \\ &\quad - A\,\mathrm{abs}\left(\delta_j^{(1)}\right) \times\int_{t=0}^{T_c} p_{T_w}\left(t-\frac{\mathrm{sgn}\left(\delta_j^{(1)}\right)T_c}{2}\right)p_{T_w}\left(t-\frac{T_c}{2}\right)dt. \end{aligned}$$

In order that the first and second terms of the above equation are nonzero, $\delta_j^{(1)}$ must be negative and positive, respectively. Since $\mathrm{abs}(x) \triangleq \begin{cases} x & x\ge 0 \\ -x & x<0 \end{cases}$, in either case, I is simplified to

$$\begin{aligned} I &= -\,\delta_j^{(1)} A \int \left(p_{T_w}(t)\right)^2 dt \\ &= -\,\delta_j^{(1)} \end{aligned}$$

where $A\int\left(p_{T_w}(t)\right)^2 dt$ has been considered to be one (normalization assumption). Thus

$$u = -\sum_{j=0}^{w-1}(-1)^{W_j^{(1,1)}}\delta_j^{(1)}. \tag{45}$$

From (14), note that

$$\begin{aligned} \delta_j^{(k)} &= n_j^{(k)} - m_j^{(k)} \\ &= \sum_{q=1}^{N^{(k)}} W_j^{(k,q)}\oplus d_j^{(k,q)} - \sum_{q=1}^{N^{(k)}}\left(1-W_j^{(k,q)}\oplus d_j^{(k,q)}\right) \\ &= \sum_{q=1}^{N^{(k)}}\left(2W_j^{(k,q)}\oplus d_j^{(k,q)}-1\right) \\ &= -\sum_{q=1}^{N^{(k)}}(-1)^{W_j^{(k,q)}\oplus d_j^{(k,q)}} \end{aligned} \tag{46}$$

where $n_j^{(k)}$ and $m_j^{(k)}$ are defined in Section II-D. Substituting $\delta_j^{(1)}$ from (46) into (45), we obtain

$$\begin{aligned} u &= \sum_{q=1}^{N^{(1)}}\sum_{j=0}^{w-1}(-1)^{W_j^{(1,1)}}(-1)^{W_j^{(1,q)}\oplus d_j^{(1,q)}} \\ &= \sum_{q=1}^{N^{(1)}}\sum_{j=0}^{w-1}(-1)^{W_j^{(1,1)}}(-1)^{W_j^{(1,q)}}(-1)^{d_j^{(1,q)}} \\ &= \sum_{q=1}^{N^{(1)}}(-1)^{D_0^{(1,q)}}\sum_{j=0}^{w-1}(-1)^{W_j^{(1,1)}}(-1)^{W_j^{(1,q)}}. \end{aligned}$$

From the orthogonality of Walsh codes, we have

$$\sum_{j=0}^{w-1}(-1)^{W_j^{(1,1)}}(-1)^{W_j^{(1,q)}} = \begin{cases} w, & q=1 \\ 0, & \text{otherwise.} \end{cases}$$

Thus, with the assumption that $D_0^{(1)}=0$, we obtain $u=w$, and the CF of the desired user signal is the same as the previous method with zero interference from the undesired services of user one. Then, we have

$$\Phi^{(1)}(s) = \exp(ws). \tag{47}$$

It can be easily shown that, for the chip-synchronous case, the CF of the interference from the interfering users is as given by (35), described in Section III-C. For this scheme, also, it is possible to derive the CF for half-chip synchronous networks, for which the result simply reduces to the result obtained for chip synchronous case, i.e., (35).

General Case: As in the previous method, when the shot-noise is taken into account, the interference from the undesired services of user 1 is not zero even though their Walsh codewords are mutually orthogonal. Consider (44). To compute the CF of the user 1, we note that w pulses (for $j=0$ to $w-1$) are

$$u = A\int_{t=0}^{wT_f}\sum_{j'=-\infty}^{+\infty}\mathrm{abs}\left(\delta_{j'}^{(1)}\right)p_{T_w}\left(t-j'T_f-c_{j'}^{(1)}T_c-\frac{\mathrm{sgn}(\delta_{j'}^{(1)})T_c}{2}\right)\times\sum_{j=0}^{w-1}(-1)^{W_j^{(1,1)}}v\left(t-jT_f-c_j^{(1)}T_c\right)dt$$

$$u = \sum_{j=0}^{w-1}(-1)^{W_j^{(1,1)}}\underbrace{A\,\mathrm{abs}\left(\delta_j^{(1)}\right)\int_{t=0}^{T_c}p_{T_w}\left(t-\frac{\mathrm{sgn}\left(\delta_j^{(1)}\right)T_c}{2}\right)v(t)\,dt}_{I} \tag{44}$$

received during the bit duration. The amplitude of the pulse in the j^{th} frame is $\text{abs}\left(\delta_j^{(1)}\right)$. When $\delta_j^{(1)}$ and $(-1)^{W_j^{(1,1)}}$ have the same sign, we have a Poisson photoelectron-count with mean $\text{abs}\left(\delta_j^{(1)}\right) m_r^{(1)}$ at the correlator output, where $m_r^{(1)}$ is the mean of received photoelectron-count from a pulse with amplitude "one" of user 1. When $\delta_j^{(1)}$ and $(-1)^{W_j^{(1,1)}}$ have different signs, we have a negative of a Poisson photoelectron-count with mean $\text{abs}\left(\delta_j^{(1)}\right) m_r^{(1)}$ at the correlator output. Now define

$$\begin{aligned} X_I &= \left\{ j \left| (-1)^{W_j^{(1,1)}} \delta_j^{(1)} \geq 0; 0 \leq j < w \right. \right\}; \\ X &= \sum_{j \in X_I} \text{abs}\left(\delta_j^{(1)}\right) = \sum_{j \in X_I} (-1)^{W_j^{(1,1)}} \delta_j^{(1)} \end{aligned} \tag{48}$$

$$\begin{aligned} Y_I &= \left\{ j \left| (-1)^{W_j^{(1,1)}} \delta_j^{(1)} < 0; 0 \leq j < w \right. \right\}; \\ Y &= \sum_{j \in Y_I} \text{abs}\left(\delta_j^{(1)}\right) = -\sum_{j \in Y_I} (-1)^{W_j^{(1,1)}} \delta_j^{(1)} \end{aligned} \tag{49}$$

where X and Y are the sum of amplitude of the pulses that produce positive and negative Poisson photoelectron-counts at the correlator output, respectively. Note that X_I and Y_I make a partition for the set $\{0, 1, \ldots, w-1\}$. Conditioned on X and Y, the CF due to user 1 is

$$\Phi_{|X=x,Y=y}^{(1)}(s) = \exp\left(x m_r \left(e^s - 1\right)\right) \exp\left(y m_r \left(e^{-s} - 1\right)\right). \tag{50}$$

From Walsh codes' orthogonal property, we have

$$\begin{aligned} x - y &= \sum_{j \in X} (-1)^{W_j^{(1,1)}} \delta_j^{(1)} + \sum_{j \in Y} (-1)^{W_j^{(1,1)}} \delta_j^{(1)} \\ &= \sum_{j=0}^{w-1} (-1)^{W_j^{(1,1)}} \delta_j^{(1)} \\ &= w. \end{aligned} \tag{51}$$

We define $v = x + y$. Then, we obtain $x = (v + w)/2$ and $y = (v - w)/2$. Thus, from (50), we have

$$\begin{aligned} &\Phi_{|x,y}^{(1)}(s) \\ &= \Phi_{|v}^{(1)}(s) \\ &= \exp\left(\frac{1}{2}(v+w) m_r (e^s - 1)\right) \exp\left(\frac{1}{2}(v-w) m_r (e^{-s} - 1)\right). \end{aligned} \tag{52}$$

Consequently, the CF of user one signal is written as

$$\Phi^{(1)}(s) = \sum_v \Phi_{|v}^{(1)}(s) p_V(v) \tag{53}$$

where $V = X + Y$ is a random variable with probability function $p_V(v)$. To compute $\Phi^{(1)}(s)$, we need to compute $p_V(v)$. From (48), (49), (46), and the definition of $d_j^{(i,q)}$ given in Section II, we have

$$\begin{aligned} V &= X + Y \\ &= \sum_{j=0}^{w-1} \text{abs}\left(\sum_{q=1}^{N^{(1)}} (-1)^{W_j^{(1,q)}} (-1)^{d_j^{(1,q)}} \right) \\ &= \sum_{j=0}^{w-1} \text{abs}\left(\sum_{q=1}^{N^{(1)}} (-1)^{W_j^{(1,q)}} (-1)^{D_0^{(1,q)}} \right). \end{aligned} \tag{54}$$

That is, V is a function of data bits and Walsh codewords dedicated to active services of user one. We suggest computer simulation to compute $p_V(v)$. For this purpose, all permutations of $D_0^{(1,q)}$ and $\left\{W_j^{(1,q)}\right\}$ for $2 \leq q \leq N^{(1)}$ must be considered. Note that $D_0^{(1,1)}$ is set to zero, and without loss of generality, $\left\{W_j^{(1,q)}\right\}$ can be considered to be all zero sequence. Therefore, the number of permutations is $2^{N^{(1)}-1} \binom{w-1}{N^{(1)}-1}$, which could be very large when the code weight w or the number of active services of user one $N^{(1)}$ is high. In this case, we may randomly choose a set of data bits and Walsh codewords for the active services to compute v and then to estimate $p_V(v)$. After estimating $p_V(v)$, $\Phi^{(1)}(s)$ is computed using (53) and (52). Fortunately, $p_V(v)$ is zero for most values of v, which makes the numerical computation of $\Phi^{(1)}(s)$ much simpler. Table I lists the value of $p_V(v)$ for a few selected pairs of w and $N^{(1)}$. These values have been computed by simulations. The values of $p_v(v)$ for v's not included in the table are equal to zero. For special cases of $N^{(1)} = 1$ or $N^{(1)} = 2$, it can be simply shown that

$$p_V(v) = \begin{cases} 1, & v = w \\ 0, & \text{otherwise.} \end{cases} \tag{55}$$

To compute $\Phi^{(k)}(s)$, we first evaluate the CF of interference component in each frame j. Similar to (34), we have

$$\Phi_j^{(k)}(s) = \alpha \Phi_{j|\text{hit}}^{(k)}(s) + \beta \Phi_{j|\text{no hit}}^{(k)}(s). \tag{56}$$

It is obvious that $\Phi_{j|\text{no hit}}^{(k)}(s) = 1$. $\Phi_{j|\text{hit}}^{(k)}(s)$ is computed as $\exp\left(-\delta_j^{(k)} m_r^{(k)} (e^s - 1)\right)$ and $\exp\left(\delta_j^{(k)} m_r^{(k)} (e^{-s} - 1)\right)$ for the value of $\delta_j^{(k)}$ being negative and positive, respectively ($\delta_j^{(k)}$ was defined in Section II-E). When $\delta_j^{(k)}$ is zero there is no interference, and, as a result, the CF will be equal to the constant 1. When data bits of q services of user k are "zero" and those of the remainders are "one," we have $\delta_j^{(k)} = N^{(k)} - 2q$. Therefore,

$$\begin{aligned} \Phi_{j|\text{hit}}^{(k)}(s) &= \sum_{q=0}^{N^{(k)}} \Phi_{j|\text{hit},q}^{(k)}(s) \Pr\{q \text{ "zero" services}\} \\ &= \sum_{\substack{q=0 \\ \delta_j^{(k)} = N^{(k)} - 2q > 0}}^{N^{(k)}} \Phi_{j|\text{hit},q}^{(k)}(s) \Pr\{q\} \\ &\quad + \sum_{\substack{q=0 \\ \delta_j^{(k)} = N^{(k)} - 2q < 0}}^{N^{(k)}} \Phi_{j|\text{hit},q}^{(k)}(s) \Pr\{q\} \\ &\quad + 1 \times \Pr\left\{N^{(k)} - 2q = 0\right\} \\ &= \sum_{q=0}^{\lceil N^{(k)}/2 \rceil - 1} \Phi_{j|\text{hit},q}^{(k)}(s) \Pr\{q\} \\ &\quad + \sum_{q=\lfloor N^{(k)}/2 \rfloor + 1}^{N^{(k)}} \Phi_{j|\text{hit},q}^{(k)}(s) \Pr\{q\} \\ &\quad + \Pr\left\{q = \frac{N^{(k)}}{2}\right\}. \end{aligned} \tag{57}$$

TABLE I
VALUE OF $p_V(v)$ FOR SOME SELECTED PAIRS OF WALSH CODE LENGTHS AND NUMBER OF ACTIVE SERVICES OF THE USER

w=4, $N^{(k)}$=4	v	4	8		
	$p_V(v)$	½	½		
w=8, $N^{(k)}$=4	v	8	12	16	
	$p_V(v)$	1.0275e-1	7.945e-1	1.0275e-1	
w=8, $N^{(k)}$=8	v	8	16	20	
	$p_V(v)$	1/16	7/16	8/16	
w=16, $N^{(k)}$=4	v	16	24	32	
	$p_V(v)$	3.525e-2	9.295e-1	3.525e-2	
w=16, $N^{(k)}$=8	v	16	24	28	
	$p_V(v)$	1.4375e-4	8.1625e-3	1.7925e-2	
	v	32	36	40	
	$p_V(v)$	3.2137e-1	5.1997e-1	1.3242e-1	
w=16, $N^{(k)}$=16	v	16	32	40	44
	$p_V(v)$	4.8828125e-4	1.708984375e-2	5.859375e-2	7.8125e-3
	v	48	52	56	64
	$p_V(v)$	4.1015625e-1	2.734375e-1	2.1875e-1	1.3671875e-2

We have $\Pr\{q\} = 2^{-N^{(k)}}\binom{N^{(k)}}{q}$, thus

$$\begin{aligned}\Phi^{(k)}_{j|\mathrm{hit}}(s) &= 2^{-N^{(k)}}\sum_{q=0}^{\lceil N^{(k)}/2\rceil-1}\exp\left(\left(N^{(k)}-2q\right)m_r^{(k)}(e^s-1)\right)\binom{N^{(k)}}{q}\\ &\quad+2^{-N^{(k)}}\sum_{q=\lfloor N^{(k)}/2\rfloor+1}^{N^{(k)}}\exp\left(\left(2q-N^{(k)}\right)m_r^{(k)}\left(e^{-s}-1\right)\right)\binom{N^{(k)}}{q}\\ &\quad+2^{-N^{(k)}}\binom{N^{(k)}}{\frac{N^{(k)}}{2}} \end{aligned}\tag{58}$$

where $\binom{N^{(k)}}{N^{(k)}/2}$ is considered to be zero when $N^{(k)}$ is odd. Finally,

$$\Phi^{(k)}(s) = \left[\Phi_j^{(k)}(s)\right]^w. \tag{59}$$

Finally, the CF of dark current and thermal noise for this method are the same as (29) and (30), respectively.

IV. NUMERICAL RESULTS

In this section, we provide some numerical results to evaluate and compare the different MR/MS schemes described in this paper. Figs. 3–6 present the BER of the five discussed methods versus the number of active services per user. The FTH code length and weight are considered to be 8192 and 16, respectively, and the number of active users is 10. The services are assumed to be similar in the network, i.e., all users have the same number of active services with the same data bit rate and quality of service. Since our main objective is to compare the multiservice and multiple-access performance of the different considered methods, we neglect circuit thermal noise and photodetector dark current in numerical results, because their influence on the system performance are the same for almost all schemes as can be seen by comparing their CFs for different methods.

Fig. 3 shows the performance of the different schemes in the Ideal Case. When the number of services per user is one, all of the methods reduce to the single-service FTH system and, as expected, have the same performance. As the number of services per user increases, the methods present different performance.

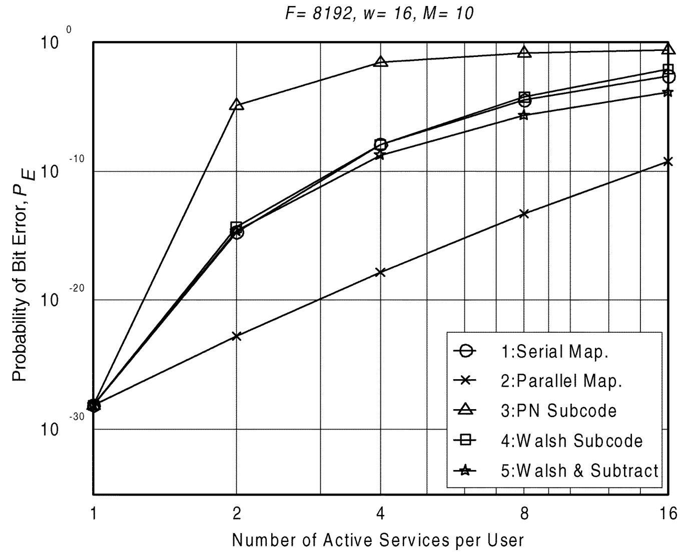

Fig. 3. BER versus number of active services per user for the five described schemes in Ideal Case. The weight and length of the FTH code is 8192 and 16, respectively, and the number of users is 10.

As it can be seen, in this case (Ideal Case), the parallel mapping method outperforms the other methods significantly as the number of services increases. Note that parallel mapping is not feasible with OOC ($\lambda = 1$) codes for the examples considered, because of its low code cardinality, however, using FTH generalized OOC, the number of codewords constraint is removed.

The multicode using PN subcode concatenation scheme (PN subcode method, for short) presents the worst multiservice performance. This poor multiservice performance is justified by the high cross correlation between the codewords of the random PN sequence dedicated to different services of the same user. This effect can be more significantly realized by comparing the results to the performance of the fourth method, where we employ orthogonal Walsh codewords to differentiate the services.

The other three methods, namely, variable spreading rate (serial mapping) method, multicode using Walsh subcode concatenation scheme (Walsh subcode method, for short), and multicode using Walsh subcode and difference modulation method (Walsh and subtract method, for short) present a fairly good performance in the Ideal Case. Among these three schemes, the Walsh and subtract method shows the best performance. The BER of this method for 16 services per user is as low as 1.24×10^{-4}, which is one twentieth of the serial mapping method and one sixtieth of the Walsh subcode method. Note that the "multiservice" interference of Walsh subcode method and Walsh and subtract method are the same, however, the Walsh and subtract method is superior to Walsh subcode method due to the reduced "multiple-access" interference.

Figs. 4–6 show the performance of the systems when the photodetector shot-noise effect is considered. Since the effect of shot noise on the optical system performance is a function of the received energy, for a fair comparison among the systems, in these figures it is assumed that the energy per service bit is the same for all the methods. Therefore, the mean received photoelectron count per pulse, denoted by m_b, is the same for all the methods. For methods one to four, w pulses are sent for each

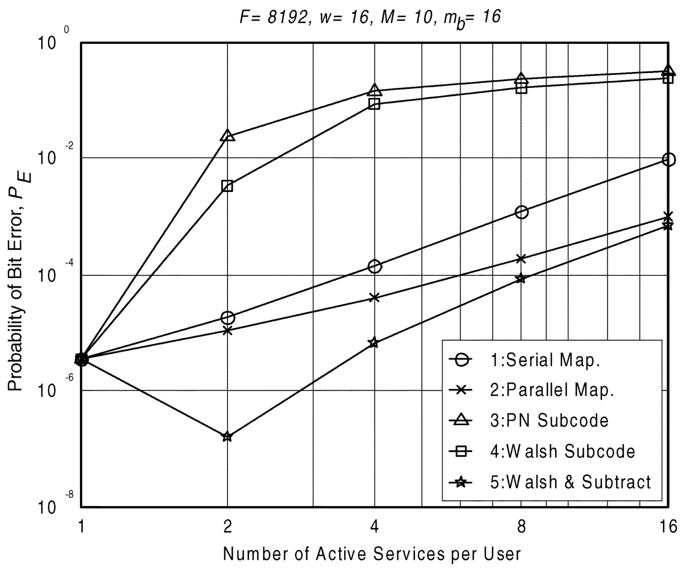

Fig. 4. BER versus the number of active services per user for the five described schemes considering photodetector shot-noise. The weight and length of the FTH code is 8192 and 16, respectively, the number of users is 10, and the mean photoelectron count per service bit is 16.

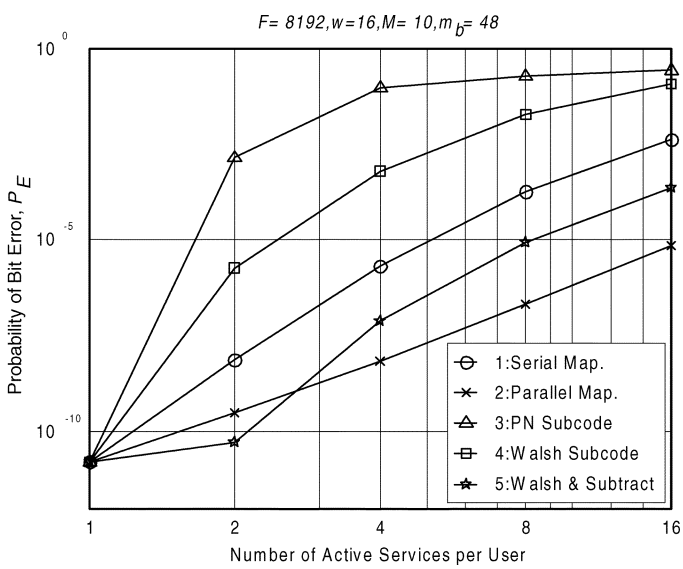

Fig. 5. BER versus the number of active services per user for the five described schemes considering photodetector shot-noise. The weight and length of the FTH code is 8192 and 16, respectively, the number of users is 10, and the mean photoelectron count per service bit is 48.

service-bit and the mean received photoelectron count per pulse is $m_r = m_b/w$. For the last method, *i.e.,* Walsh and subtract method, the mean received photoelectron-count from user k in w frames, $m_b^{(k)}$, is computed as

$$m_b^{(k)} \triangleq \mathbb{E}\left\{m_r^{(k)} V\right\} = m_r^{(k)} \sum_v v p_V(v) \tag{60}$$

where V is defined in (54) and $m_r^{(k)}$ is the mean received photoelectron count per pulse with amplitude "one" from user k and $\mathbb{E}\{\cdot\}$ is the expectation operator. On the other hand, from the

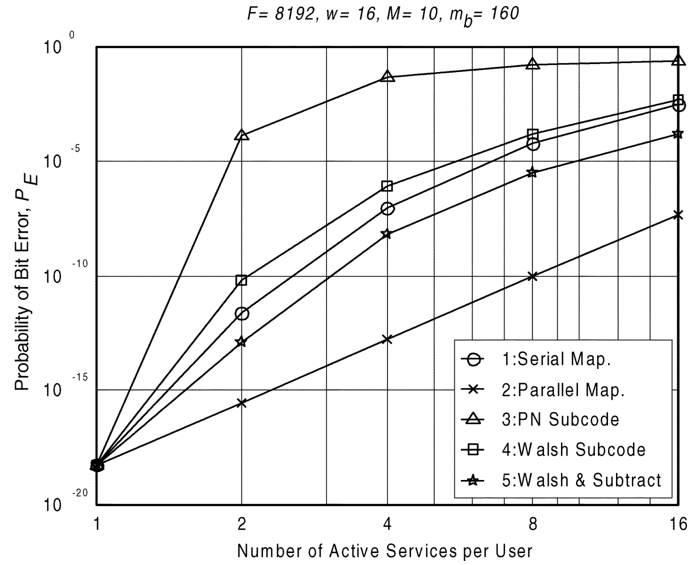

Fig. 6. BER versus the number of active services per user for the five described schemes considering photodetector shot-noise. The weight and length of the FTH code is 8192 and 16, respectively, the number of users is 10, and the mean photoelectron count per service bit is 160.

definition of m_b given above, for user k with $N^{(k)}$ active services, the total received photoelectron count is $N^{(k)} m_b$. Therefore, we have

$$m_r^{(k)} = \frac{N^{(k)} w m_r}{\sum_v v p_V(v)} \triangleq \kappa m_r \tag{61}$$

where κ is the power efficiency factor. That is, for the same transmitting energy per service bit, the pulses are κ times stronger in the Walsh and subtract method compared to the other methods. Therefore, assuming a Poisson photoelectron count, the signal-to-shot-noise ratio is increased by a factor of κ compared to other methods. It can be shown that

$$\kappa = \begin{cases} \dfrac{2^{N^{(k)}-1}}{\binom{N^{(k)}-1}{\frac{N^{(k)}}{2}}}, & N^{(k)} \text{ even} \\ \dfrac{2^{N^{(k)}-2}}{\binom{N^{(k)}-2}{\frac{(N^{(k)}-1)}{2}}}, & N^{(k)} \text{ odd.} \end{cases} \tag{62}$$

Using Stirling's formula for factorial $(n! \underset{n\to\infty}{\longrightarrow} \sqrt{2\pi n} n^n \times \exp(-n))$, we get

$$\kappa \approx \sqrt{\frac{N^{(k)}\pi}{2}}. \tag{63}$$

As can be realized, the power efficiency factor is proportional to the square root of the number of active services of the user. From Fig. 4, in which the received power is low and the shot-noise effect is at a maximum, the Walsh and subtract method presents the best performance among the considered methods.

As can be seen from this figure, when the number of active services increases from one to two, the BER of the Walsh and subtract method decreases. This phenomenon is explained as follows: The noise at the receiver is the sum of the photodetector shot-noise, and multiservice and multiple-access noise. When the received power is low, the dominant noise is the shot noise. From (62), the signal to shot-noise ratio is increased by a factor of 2, when the number of services increases from one to two, assuming a constant energy per service bit. Moreover, it can be shown that the desired user's multiservice noise is "zero" for this scheme when the number of services is two [(55) and Fig. 2(e)]. As a result, the BER decreases when the number of services increases from one to two. As the number of services increases to higher values, however, multiple-access and multiuser noise dominate the received noise and, despite the decrement of the shot-noise effect, BER increases.

By increasing the power (Figs. 5 and 6), the results tend to that of the Ideal Case. For instance, in Fig. 5, in which the received power is relatively higher than that in Fig. 4, even though the Walsh and subtract method presents a superior performance than the parallel mapping method for two active services per user, the parallel mapping method performs better for a higher number of active services. We can justify the results in the following way: when the number of active services is small, as mentioned before, the dominant source of noise is the photodetector shot noise and, as a result, the Walsh and subtract method presents a better performance. On the other hand, when the number of active services is high, the dominant source of noise is the multiple-access noise. Therefore, the results are the same as in the Ideal Case, in which parallel mapping presents the best performance. When the received power is high, as in Fig. 6, the shot noise has a minimum effect, and the results are similar to the results of the Ideal Case.

V. Conclusion

In this paper, we studied multirate/multiservice methods for optical CDMA networks based on FTH generalized OOC codes. Two well-known MR/MS schemes, namely, serial mapping (or variable spreading rate) and parallel mapping methods, and three newly proposed schemes based on multicode using subcode concatenation scheme were considered. In the three new schemes, users are separated using dedicated FTH codewords, however, different services of a user are differentiated using a binary subcode (e.g., binary PN or Walsh codes). FTH patterns present a high code cardinality which is very desirable in MR/MS applications. Moreover, the proposed multicode schemes present high flexibility for supporting MR/MS applications such as simpler coordination protocols, simpler service synchronization, and lower implementation complexity and cost.

Performance analysis was done by computing the characteristic function of decision variables and employing saddle-point approximation techniques. Numerical results have shown that the parallel mapping scheme outperforms the other schemes significantly when the received power is high (i.e., the Ideal Case). On the other hand, when the received power is low the method of multicode using Walsh subcode and difference modulation presents the best performance. In this method, different services of a user have a minimal interference on each other. Furthermore, the variance of photodetector shot noise is reduced by a factor proportional to square root of number of active services of the user.

Acknowledgment

The authors would like to thank Dr. M. Abtahi, E. Karami, and Prof. J. Salehi for their support and helpful comments.

References

[1] J. A. Salehi, "Code division multiple-access techniques in optical fiber network–Part I: Fundamental principles," *IEEE Trans. Commun.*, vol. COM-37, no. 8, pp. 824–833, Aug. 1989.
[2] J. A. Salehi and C. A. Brackett, "Code division multiple-access techniques in optical fiber network–Part II: System performance analysis," *IEEE Trans. Commun.*, vol. COM-37, no. 8, pp. 834–842, Aug. 1989.
[3] A. Stok and E. H. Sargent, "The role of optical CDMA in access networks," *IEEE Commun. Mag.*, vol. 40, no. 9, pp. 83–87, Sep. 2002.
[4] J. Ratnam, "Optical CDMA in broadband communication-scope and applications," *J. Opt. Commun.*, vol. 23, no. 1, pp. 11–21, Jan. 2002.
[5] S. V. Maric, O. Moreno, and C. J. Corrada, "Multimedia transmission in fiber-optic LAN's using optical CDMA," *J. Lightwave Technol.*, vol. 14, no. 10, pp. 2149–2153, Oct. 1996.
[6] J. G. Zhang, "Design of a special family of optical CDMA address codes for fully asynchronous data communications," *IEEE Trans. Commun.*, vol. 15, pp. 452–457, 1997.
[7] ——, "Novel optical fiber code-division multiple access networks supporting real-time multicahnnel variable-bit-rate (VBR) video distortions," *IEEE Trans. Broadcast*, vol. 43, no. 3, pp. 339–348, Sep. 1997.
[8] W. C. Kwong and G. C. Yang, "Design of multilength optical orthogonal codes for optical CDMA multimedia networks," *IEEE Trans. Commun.*, vol. 50, no. 8, pp. 1258–1265, Aug. 2002.
[9] S. V. Maric and K. N. Lau, "Multirate fiber-optic CDMA: System design and performance analysis," *J. Lightwave Technol.*, vol. 16, no. 1, pp. 9–17, Jan. 1998.
[10] H. Yashima and T. Kobayashi, "Optical CDMA with time hopping and power control for multimedia networks," *J. Lightwave Technol.*, vol. 21, no. 3, pp. 695–702, Mar. 2003.
[11] A. R. Forouzan, J. A. Salehi, and M. Nasiri-Kenari, "Frame time-hopping fiber-optic code division multiple-access using generalized optical orthogonal codes," *IEEE Trans. Commun.*, vol. 50, no. 12, pp. 1971–1983, Dec. 2002.
[12] C.-L. I and R. D. Gitlin, "Multicode CDMA wireless personal communications networks," in *Proc. IEEE Int. Conf. Commun.*, Seattle, WA, Jun. 1995, pp. 1060–1064.
[13] C. W. Helstrom, "Approximate evaluation of detection probabilities in radar and optical communications," *IEEE Trans. Aerosp. Electron. Syst.*, vol. AES-14, no. 7, pp. 630–640, Jul. 1978.
[14] G. Durisi and S. Benedetto, "Performance evaluation of TH-PPM UWB systems in the presence of multiuser interference," *IEEE Commun. Lett.*, vol. 7, no. 5, pp. 224–226, May 2003.

Amir R. Forouzan (S'99) received the B.S. and M.S. degrees in electrical engineering from the Sharif University of Technology (SUT), Tehran, Iran, in 1998 and 2000, respectively, and Ph.D. degree in electrical engineering from the University of Tehran, Tehran.

From 1999 to June 2001, he was with the Technical Staff of Advanced Communication Science Research Laboratory, Iran Telecommunication Research Center (ITRC), Tehran, and, from July 2001 to May 2004, he was with the Mobile Communications Division, ITRC. Since June 2004, he has been a Postdoctoral Fellow with the University of Canterbury, Christchurch, New Zealand, working on MIMO techniques in digital subscriber lines and MIMO information theory. His research interests include optical CDMA, MIMO communication systems and information theory, and ultrawideband radio.

Masoumeh Nasiri-Kenari (S'89–M'94) received the B.S and M.S. degrees in electrical engineering from the Isfahan University of Technology, Isfahan, Iran, in 1986 and 1987, respectively, and the Ph.D. degree in electrical engineering from the University of Utah, Salt Lake City, in 1993.

From 1987 to 1988, she was a Technical Instructor and Research Assistant with the Isfahan University of Technology. Since 1994, she has been with the Department of Electrical Engineering, Sharif University of Technology, Tehran, Iran, where she is now a Professor. She is also the Director of Wireless Research Laboratory of the Electrical Engineering Department. From 1999 to 2001, she was a Co-Director of the Advanced Communication Science Research Laboratory, Iran Telecommunication Research Center, Tehran. Her current research interests are in wireless communication systems and error correcting codes.

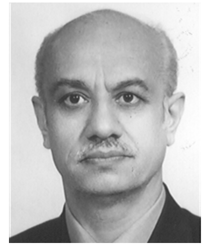

Nasser Rezaee (S'75–M'80) received the M.Sc. degree in electrical engineering from the University of Tehran, Tehran, Iran, in 1970, and the M.Sc. and Ph.D. degrees in telecommunications systems from the University of Essex, Essex, U.K., in 1976 and 1980, respectively.

Since 1980, he has been a member of the Department of Electrical and Computer Engineering, University of Tehran, where he is currently an Associate Professor of telecommunications systems. In 1971, he was a Visiting Researcher with the NTT Electrical Communication Laboratories, Japan, where he was involved in the early studies of high-bit-rate digital transmission systems. During 1971–1975, he was with the Iran Telecommunication Research Centre (ITRC), Tehran, where he was involved in design and implementation of transmission systems. He is the author of the book *Transmission Systems for Communications* (Tehran, Iran: Tehran University Press, 1994). He has published many papers in international journals and conferences. His main areas of interest are architectural and system aspects of optical networks and cellular mobile networks.